



Structural changes of chromatin fibers induced by variation of linker DNA length

THESIS

submitted in partial fulfillment of the
requirements for the degree of

MASTER OF SCIENCE
in
PHYSICS

Author : Margherita Botto
Student ID : s1731165
Supervisor : T. B. Brouwer, prof. dr. ir. S. J. T. van Noort
2nd corrector : prof. dr. Helmut Schiessel

Leiden, The Netherlands, October 9, 2017

Structural changes of chromatin fibers induced by variation of linker DNA length

Margherita Botto

Huygens-Kamerlingh Onnes Laboratory, Leiden University
P.O. Box 9500, 2300 RA Leiden, The Netherlands

October 9, 2017

Abstract

In this thesis we are going to study the mechanical properties of a chromatin fiber. Chromatin is the second compaction stage of DNA, after the wrapping of DNA around histones proteins to form nucleosomes. Specifically we are going to analyze how its behaviour under external stresses is going to change with the variation of the linker DNA length, the DNA segment that links two adjacent nucleosomes. We will be able to do it at a single-molecule level thanks to the use of magnetic tweezers, an apparatus that can exert forces and torques directly to individual molecules.

Acknowledgements

I would like to thank John van Noort, Thomas Brouwer, Artur Kaczmarczyk, Nicolaas Hermans and Chi Pham for the stimulating discussions and helpful suggestions. I would like to offer my special thanks to Thomas Brouwer and Artur Kaczmarczyk for the courtesy of their experimental data (167, 197 and 202 NRL fibers).

Contents

1	Introduction	1
2	Theory	5
2.1	DNA mechanics	5
2.2	Chromatin mechanics	7
2.2.1	Free energy of the first transition	8
3	Materials and methods	15
3.1	Samples	15
3.1.1	Chromatin reconstitution	15
3.2	Magnetic Tweezers	19
4	Results	21
4.0.1	Comparison between chromatin fibers	21
4.1	Analysis	25
4.1.1	Torsionally free and torsionally constrained 172 NRL fibers	27
4.2	192 NRL fiber	30
5	Discussion	32
5.1	172 NRL fiber	32
5.1.1	Torque effects on 172 NRL fibers	33
5.2	Does the experimental ΔG_1 agree with theory?	35
6	Conclusion	37

Chapter 1

Introduction

Deoxyribonucleic acid, DNA, carries genetic instructions for the growth, development, function and reproduction of all living organisms. DNA molecules are long biopolymers. The human genome contains [15] 6×10^9 base pairs, leading to almost 2 meters of length. Molecules of such size can not fit into cell nucleus without the right packaging.

DNA passes through multiple compaction levels (see figure 1.1 A) forming chromatin structure. In chromatin, DNA is coiled tightly together with histone proteins *H3*, *H4*, *H2A* and *H2B*. Packaging of DNA into chromatin plays an important role in many biological processes and is most extreme during mitosis and meiosis, when the cell divides [16]. As the cell enters in one of these two states, the chromatin segregates into chromosomes. Chromatin prevents chromosome breakage [17] and controls gene expression and DNA replication [18]. Therefore, chromatin is essential for life. Yet its structure is not completely understood.

The first level of DNA compaction consists of an array of nucleosomes connected by short DNA segments, the linker DNA. A nucleosome is made by wrapping DNA 1.7 times around eight histone protein core (one *H3* – *H4* tetramer and two *H2A* – *H2B* dimers) [21]. Every nucleosome wraps 147 bp of DNA. The resulting structure is shown in figure 1.1 B. In the next level of condensation nucleosomes stack together, forming a higher order structure, referred to as a 30 nm fiber. Depending on the length of the linker DNA the nucleosomes will have a different rotational and translational position. This could induce a different shape in the higher order structure of the chromatin.

In such regular fibers the length of the linker DNA is defined by the repeat length, geometrically referred to as the nucleosome repeat length. It consists of the sum of the linker DNA length and the 147 bp wrapped

around the nucleosomes. Chromatin fibers can be reconstituted on DNA containing repeats of the Widom 601 sequence. The three fibers that are schematically depicted in figure 1.2 differ in their NRLs. Both 167 and 197 NRL constructs show the same nucleosomes orientation relative to the DNA. In contrast the construct for the 172 NRL fibers (figure 1.2 B), with 25 bp of linker DNA, shows translation and rotation between adjacent nucleosomes.

Since every 10.4 bp the two strands forming DNA twist around their helical axis, the two nucleosome-spacing categories will show different spacial organization. Recent studies [20, 22, 23] show that distinctive periodicity of nucleosomes also occur in nature. Initially, the nucleosomes spacing of integer multiples of ten ($10n$) were reported. More recent work, making use of modern high resolution sequencing methods, suggests nucleosomes spacing of $10n + 5$ are more common. The research topic of this thesis will be how this difference will affect the higher order of chromatin structure.

Two groups of competing models have been proposed to explain higher-order chromatin structure, the "one start" solenoid model and the "two start" zig-zag model [19]. In the solenoid model consecutive nucleosomes interact with each other following a helical trajectory. In the zig-zag model two columns of nucleosomes twist into a double helix, so that alternate nucleosomes can interact. For the 167 NRL fiber the zig-zag structure has been theorized and widely proven [5, 6, 19, 22, 23], while for the 197 NRL a solenoid structure has been proposed [5, 6]. While the structures for the 167 and 197 NRL fibers have been studied thoroughly, the 172 NRL is relatively unexplored. However, Nikitina et al. in [14] propose an anti-parallel zig-zag model for the 172 NRL fiber.

Here, we will compare the mechanical behaviour of different chromatin fibers using single-molecule force spectroscopy. We will focus on the transition that ruptures the fibers into a beads-on-a-string configuration. Experiments are performed by pulling the chromatin fibers with a magnetic tweezers setup. Furthermore, we will analyse the effects of torsion on a chromatin fiber by comparing the behaviour of a torsionally free and torsionally constrained fiber.

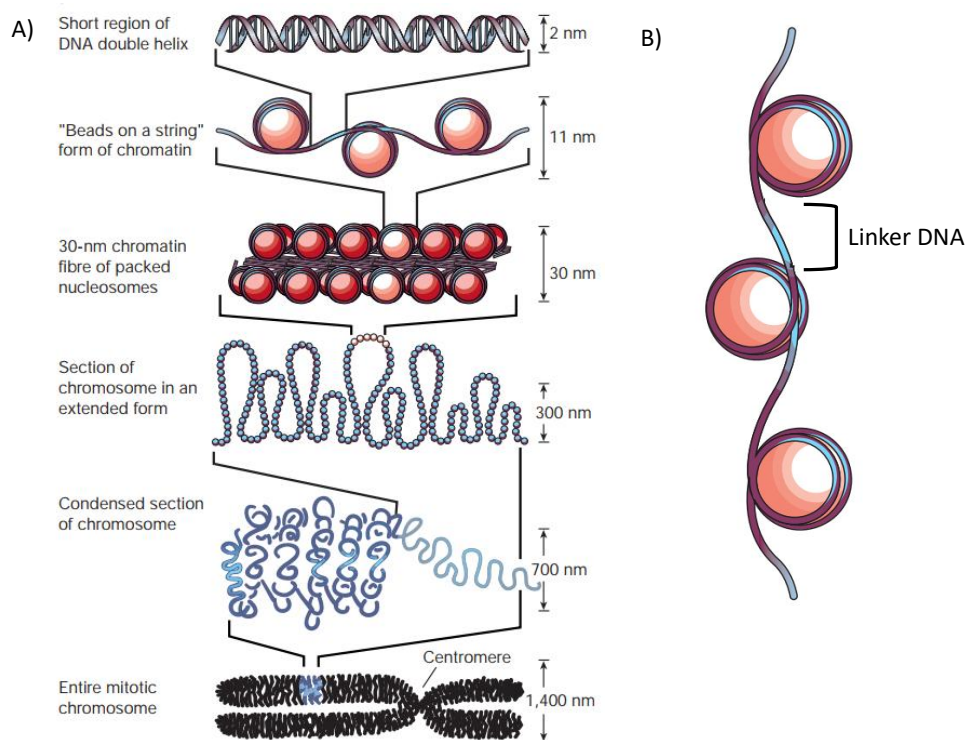


Figure 1.1: The compaction of DNA consists of multiple levels, the 2nm DNA helix, the 11nm beads-on-a-string, the 30nm chromatin fiber, the 300nm section of a chromosome, the the 700 nm condensed chromosome section and the 1,400nm entire chromosome A) Schematic view of the levels of compaction that from bare DNA lead to the creation of a chromosome. B) Zoom in on the first compaction level. 147 bp of DNA wrap around a core of eight histones forming nucleosomes, separated by the linker DNA. Images taken from [1].

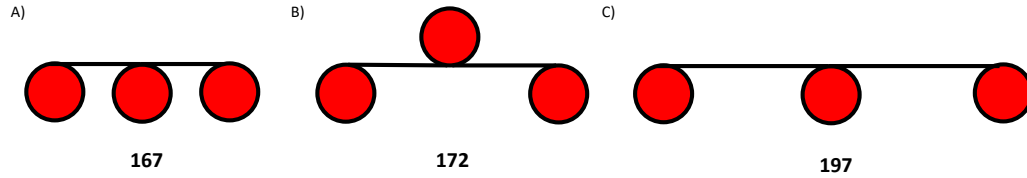


Figure 1.2: Linker length variations induce orientational offset between nucleosomes. This will lead to differences in the fiber structure. Every 10.4 DNA bp the two strands twist around the helical axis. Thus, structures with linker DNA length of $10n$ would be different than the ones with a linker length of $10n+5$ A)167 NRL. For a linker DNA of 20 bp a zig-zag structure has been proposed and also widely confirmed. B)172 NRL. Linker DNA of 25 bp. C)197 NRL. For a linker DNA of 50 bp a solenoid structure has been proposed.

Theory

2.1 DNA mechanics

In order to be able to understand the mechanical properties of a chromatin fiber we should start by understanding those of a double stranded DNA molecule. DNA is a flexible polymer that is subject to thermal fluctuations when in solution. Therefore, it functions as an entropic spring. At room temperature the distance between the two ends of the chain will be significantly shorter than the contour length L_0 . Stretching the molecule prohibits states with high curvatures and hence small extensions lead to a decrease in entropy and an increase of free energy of the entire molecule [4]. To describe the DNA chain flexibility we use a model called the Worm Like Chain (WLC). This model describes the double stranded DNA as an isotropic rod that is continuously flexible [3].

In order to analyse the possible states available for our DNA molecule, we consider Boltzmann's law (equation 2.1). We can then see that the states characterized with the lowest free energy (G) have the highest probability to happen.

$$P(x) \propto e^{\frac{-G(x)}{k_B T}} \quad (2.1)$$

Upon stretching the DNA the accessible spectrum of fluctuations reduces, causing the raise of an "entropic force" against external elongation. In absence of external forces this entropic force tends to collapse the chain on itself, trying to make the distance between the two free ends as short as possible. The entropy of a system is described by equation 2.2.

$$S = k_B \ln w \quad (2.2)$$

where k_B is the Boltzmann constant and w represents the number of configurations available for each state. Equation 2.3 relates the energy of the system to the Gibbs free energy G :

$$G = E - TS \quad (2.3)$$

in which E represents the internal energy of the system and T is the temperature.

To derive an expression for the extension of a DNA molecule as a function of force, an entropic term representing bending fluctuations and a work term are considered [5]:

$$G(f) = G_{entropic} + G_{external} = \frac{1}{2}k_B T \int_0^{L_0} P \frac{\delta^2 r(s)}{\delta s^2} ds - fz \quad (2.4)$$

To calculate the force needed to stretch the molecule, one should minimize the free energy for each force. A useful approximation was derived by J.F.Marko and E.D. Siggia [4]:

$$F = \frac{k_B T}{A} \left(\frac{1}{4(1 - \frac{z}{L_0})^2} - \frac{1}{4} + \frac{z}{L_0} \right) \quad (2.5)$$

where z is the extension and A is the persistence length of the chain and it describes the length over which correlations in the direction of the tangent to the rod itself are lost [4].

In order to be able to calculate the stretching of a DNA molecule measured with the magnetic tweezers we would need the inverse function, the extension z caused by the force F [4]:

$$z(f) = L_0 \left(1 - \frac{1}{2} \sqrt{\frac{k_B T}{fA}} \right) \quad (2.6)$$

For forces above 10 pN the compliance of the DNA along the contour must be accounted for, leading to an enthalpic energy to be considered:

$$G(f) = G_{entropic} + G_{enthalpic} + G_{external} = \frac{1}{2}k_B T \int_0^{L_0} P \frac{\delta^2 r(s)}{\delta s^2} ds + \frac{1}{2} \frac{S}{L} z^2 - fz \quad (2.7)$$

leading to:

$$F = \frac{k_B T}{A} \left(\frac{1}{4(1 - \frac{z}{L_0})^2} - \frac{1}{4} + \frac{z}{L_0} + \frac{f}{S} \right) \quad (2.8)$$

where S is the stretching modulus, that describes how DNA resists to elastic deformations induced by external stresses. The equivalent to equation 2.6 is:

$$z(f) = L_0 \left(1 - \frac{1}{2} \sqrt{\frac{k_B T}{fA} + \frac{f}{S}} \right) \quad (2.9)$$

2.2 Chromatin mechanics

When 147 base pairs of DNA wraps around a histone octamer, a nucleosome is formed. Nucleosomes form on longer stretches of DNA interactions between each others, leading to a further compaction into a chromatin fiber. The structure of the chromatin fiber is still elusive. The scientific community [9] has focused on two main chromatin structures, a two-start helix, called a zig-zag structure, and a one start helix, called a solenoid structure.

To describe how a chromatin fiber responds to force, we distinguish the different unfolding transitions through which a fiber unfolds and use a statistical mechanics model [5] to quantify different unwrapping states that lead to a fully stretched DNA strand (figure 2.1).

Starting from the folded fiber, an energy penalty of ΔG_1 is paid to unstack a pair of nucleosomes and to partially unwrap the DNA. At this point one turn of DNA remains bound around the histones (89 bp) and the fiber has become a string of single-wrapped nucleosomes. With an energy difference of ΔG_2 the single wrap unfolds to an extended extended configuration. When the last DNA unwraps from the tetrasome core, the extension can be described by a WLC, with an addition to the free energy of ΔG_3 that is required to separate the remaining DNA from the histone core.

The extension and free energy of the entire fiber can be calculated adding the contribution of each of the nucleosomes, that can be in either of the four conformations, and the DNA handles:

$$z(f) = \sum_i n_i z_i(f) + z_{DNA}(f) \quad (2.10)$$

$$G(f) = \sum_i n_i G_i(f) + G_{DNA}(f) \quad (2.11)$$

The number of states in which the fiber can be found is large but finite. To simplify computation, this number can be reduced by grouping the states that have the same number of nucleosomes in each conformation, but in

a different order. Because we recognize different states from the extension of the fiber, those grouped states will be not distinguished between each other. We can include all of them in our calculations by including a degeneracy factor D :

$$D(\text{state}) = \prod_{i < j} \binom{n_i + n_j}{n_i} \quad (2.12)$$

where i and j represent the different pairs of conformations in each state.

Thus the mean equilibrium extension can be calculated as:

$$\langle z_{TOT}(f) \rangle = \frac{\sum_{\text{states}} z(f) D(\text{state}) e^{-((G(f) - F_{z(f)})/k_B T)}}{\sum_{\text{states}} D(\text{state}) e^{-((G(f) - F_{z(f)})/k_B T)}} \quad (2.13)$$

Equation 2.13 shows the importance of the degeneracy term D . A one start helix will respond differently than a two start helix. Not only will the stiffness of the folded two-start helix containing the same number of nucleosomes be 4 times stiffer because there will be two stacks of half the height in parallel, but also the unfolding kinetics will be different. In a one-start fiber, each nucleosome pair can unstack independently, so the transition is degenerate.

In a two-start fiber on the other hand, the end nucleosomes are more fragile, as they are only stabilized by interactions with 1 neighbour. The force on embedded nucleosomes is distributed over the two stacks, which stabilizes these nucleosomes. Accordingly, zig-zag fibers will unfold from the ends, like a zip. Such cooperative unfolding is modelled by a degeneracy $D=0$.

2.2.1 Free energy of the first transition

Since the folding of the chromatin fiber, which is heavily debated, is defined by the first conformation and therefore by ΔG_1 , we decided to look more carefully into this term. It has been defined in [5] as the energy difference between stacked nucleosomes and unstacked, partially unwrapped nucleosomes.

Therefore, we split ΔG_1 into four contributions:

$$\Delta G_1 = \Delta G_S + \Delta G_B + \Delta G_T + \Delta G_U \quad (2.14)$$

ΔG_S represents the stacking energy between nucleosomes, thus their interaction energy. ΔG_B and ΔG_T are the bend and twist terms, which express

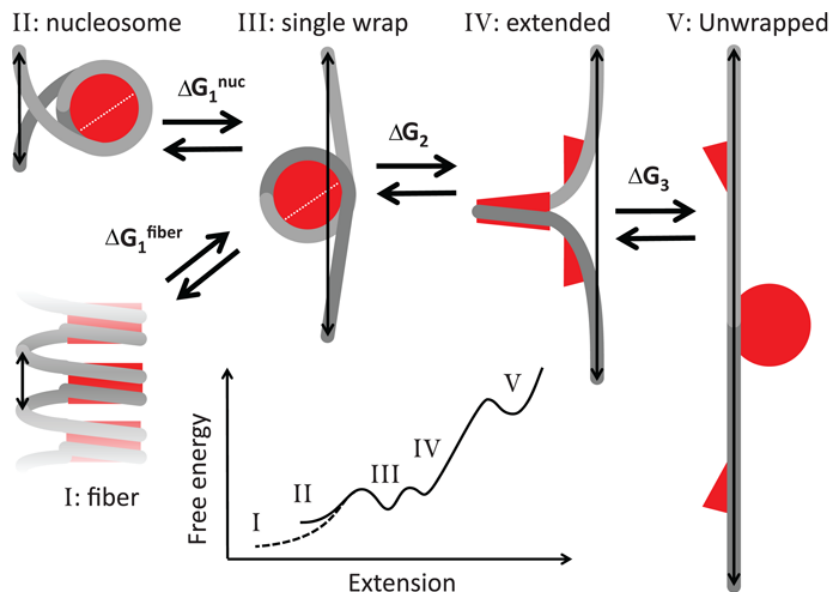


Figure 2.1: The energy landscape for unfolding chromatin fibers. The lowest energy is where the fiber is completely folded. When exposed to more force, the fiber undergoes a transition to a single wrap of DNA around the core histones and a change in the free energy ΔG_1 . As the force increases the chain experiences a small extension with an energy loss of ΔG_2 before it unwraps completely. At the end, there is the fully unfolded configuration that has a behaviour described by the worm-like-chain. The solid line at small extension represents the free energy of a single non-stacked nucleosome. Image taken from [5].

the energy to bend and twist the linker DNA. ΔG_U represents the linker DNA unwrapping energy.

In Figure 2.2 B we show a section of the solenoid structure, where the dashed lines represent the linker DNA and the solid line the DNA wrapped around the nucleosome. Multiple dashed lines indicate that different amounts of DNA can be unwrapped from the histones core while the nucleosomes remain stacked. Figure 2.2 B shows that linker DNA length can be optimized to minimize bending and twist stress imposed by the stacked nucleosomes. Thus we are now able to analyse ΔG_1 for the solenoid structure term by term.

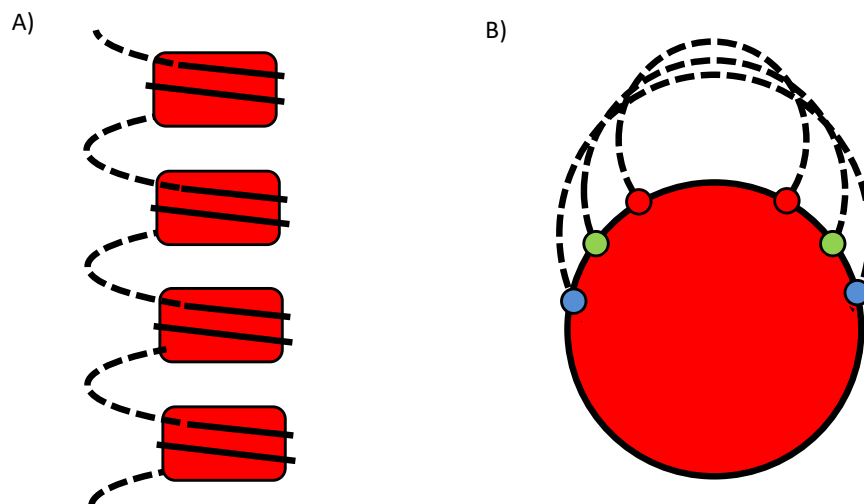


Figure 2.2: A one-start chromatin fiber can minimize twist and bend (A) by unwrapping several bases from the histone core(B). Different linker lengths will behave differently, indicating that a variation in NRL influences the fiber structure.

Since ΔG_S is equal for all stacked configurations, irrespective of the NRL of the fiber, we will treat it as a constant. We are only interested in differences between stacked conformations, so we will set it to zero. Subsequently for each base pair unwrapped the ΔG_U increases with 0.2

kT [5]. We model the DNA strand as a flexible rod, and calculate the ΔG_B using the formula for the elastic energy of a simple rod [3, 8]

$$\frac{\Delta G_B}{k_B T} = \frac{A(l + u)}{2r^2} \quad (2.15)$$

where A is the bending persistence length, l is the length of the linker DNA, u is the number of unwrapped base pairs and r is the radius of the semi-circumference describing the linker DNA.

The term to calculate for the bending energy is the radius r . We started with the calculation of β , shown in figure 2.3:

$$\beta = \left(\frac{l_{free} + u}{l_{wrap}} \right) 2\pi \quad (2.16)$$

where l_{free} represents the amount of base pairs that would be needed to fill the gap between the two ends of the nucleosomal DNA around the circumference of the nucleosome. l_{wrap} is the number of base pairs of a complete turn of DNA around the nucleosome.

Then we calculated d , the red segment in Figure 2.3:

$$d = R \sin \frac{\beta}{2} \quad (2.17)$$

where R is the radius of the nucleosome (± 4.5 nm)[2, 8].

For the radius r of the linker segment there are two solutions depending on the linker length.

$$\begin{cases} \text{if } l < \pi d & l + u = \theta r \\ \text{if } l \geq \pi d & l + u = (2\pi - \theta)r \end{cases} \quad (2.18)$$

where $\pi d = 68$ bp. Combining 2.17 and 2.18 yields:

$$l + u = \theta \frac{d}{\sin \frac{\theta}{2}} \quad \text{or} \quad l + u = (2\pi - \theta) \frac{d}{\sin \frac{\theta}{2}} \quad (2.19)$$

which can be solved for θ . Then we can calculate r :

$$r = \frac{d}{\sin \frac{\theta}{2}} \quad (2.20)$$

Once we finally have r we can calculate ΔG_B .

The energy stored in the twist, ΔG_T , is:

$$\Delta G_T = \frac{1}{2} c \sigma^2 (l + u) \quad (2.21)$$

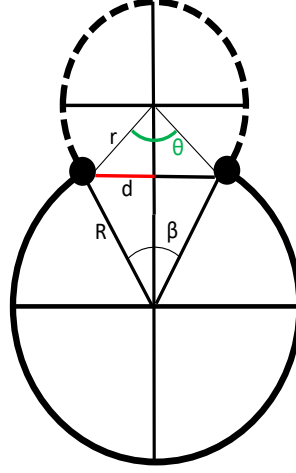


Figure 2.3: A simplified model for a nucleosome and its linker DNA in the solenoid structure.

where c is the twist modulus, defined as:

$$c = k_B T \omega_0^2 C \quad (2.22)$$

C is the twist persistence length ($C_{twist} = 100$ nm) and ω_0 is the intrinsic twist, defined as $\omega_0 = \frac{2\pi}{3.6\text{nm}} = 1.75\text{nm}^{-1}$ where 3.6 nm is the helix repeat distance. The σ in equation 2.21 is called the twist density and is defined as:

$$\sigma = \frac{\Delta Lk}{Lk_0} = \frac{\theta}{\frac{2\pi}{n_h}} \quad (2.23)$$

where Lk_0 is the linking number and equals 1 helical turn per 10.4 bp for B-DNA. ΔLk represents the change in linking number after imposing to the structure some torsional stress. n_h represents the number of base pairs that forms an helix turn of the DNA with no stress applied to the strand. θ represents the twist angle applied to the DNA. Since we do not know the exact geometrical constraints that are imposed on the linker DNA by nucleosome-nucleosome stacking, we evaluate two extreme cases. If the geometry is optimal, no torsional stress is imposed, i.e. $\theta=0$. In the worst case scenario, half a turn of twist needs to be distributed in the linker DNA, so $\theta=\pi$. We calculated all the values of the energies composing ΔG_1 for the two extreme cases for linker lengths between 25 and 55 bp in steps of five

(figure 2.4 shows the results for $\theta=\pi$). We notice that the plot for the bending energy ΔG_B shows that the 25 bp fiber has a distinct linear behaviour. This is because this configuration has a linker length that does not need additional bending energy to connect two nucleosomes. It perfectly supplements the 61 bp of the last not-complete turn of DNA around the histones in order to arrive at 86 bp, the amount of base pairs needed for a complete turn of DNA around the histones core. Using equation 2.14 we calculated the total ΔG_1 , shown in the two graphs in Figure 2.5 both for 0° and 180° twist.

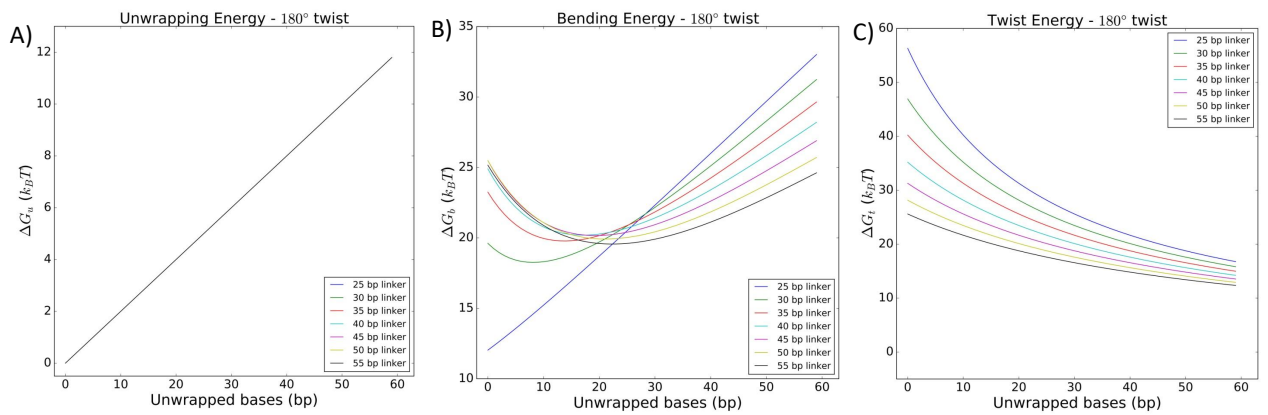


Figure 2.4: DNA unwrapping minimalizes the free energy of nucleosome stacking. Differences in twist energy can be large for various conformations.

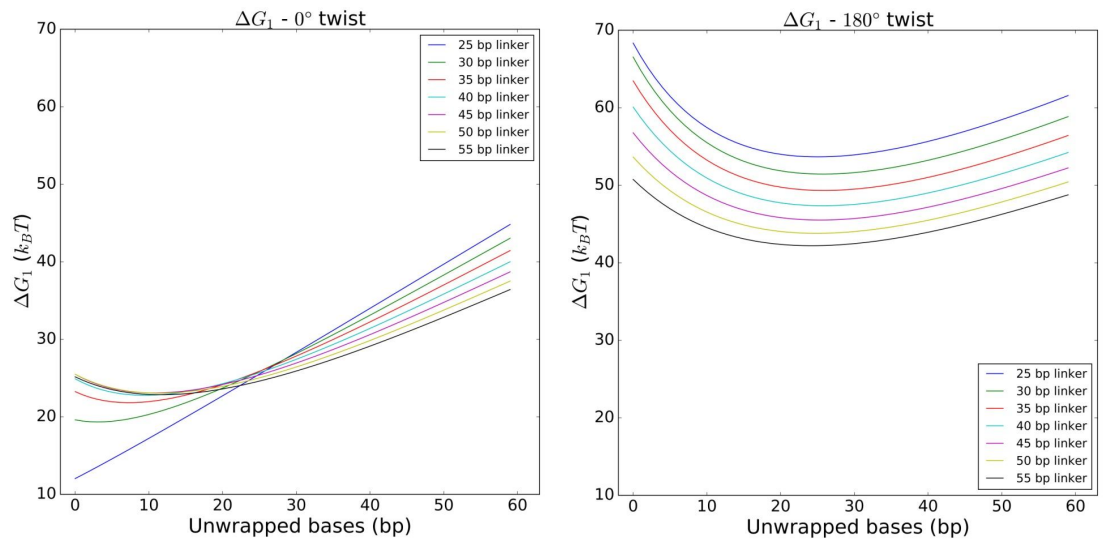


Figure 2.5: Independent ΔG_1 graphs show a energy free minimum around 15-20 base pairs. However for a 180° twisted linker DNA the free energy is much higher because of the twist term in equation 2.14.

Materials and methods

3.1 Samples

To reconstitute a chromatin fiber we start from a plasmid pUC19 DNA with tandem repeats of the 601 Widow sequence. We used this specific sequence because this substrate results in very regular fibers that have a well-defined linker length [12].

For our experiments we want to end up with a DNA construct with ends labelled with the biochemical linkers biotin and digoxigenin to attach one end of our construct to a streptavidin(SA)-coated magnetic bead (using biotin) and the other end to the anti-dig(AD)-coated glass surface of a flow cell (using digoxigenin). The procedure used to digest and label the plasmid is visible in Table I.

As shown in figure 3.1 A plasmid is digested at two different sites in two consecutive steps and filled in with modified bases using two Klenow reactions. In figure 3.1 A we can see the gel representing each of those steps. Figure 3.1 B shows a schematic representation of our final product, where we can see the labels at the edges and the 601 sequence repetitions in the middle.

For the torsionally constrained substrate we ligated two DNA handles (green in figure 3.1 C) of 650 bp each with multiple labels of biotine (bio) and digoxigenin (dig) to the 601 array.

3.1.1 Chromatin reconstitution

Once the DNA constructs have been prepared we start with the chromatin reconstitution [13]. We add octamers to the DNA construct in six different octamer-DNA ratios. Then we put our six samples on dialysis membranes

Step n°	Materials	Process
1	<ul style="list-style-type: none"> • pUC19 DNA plasmid • BseYI enzyme • 3.1 NEB buffer • MQ 	pUC19 digestion. Incubate at 37° overnight
2	<ul style="list-style-type: none"> • BseYI-digested pUC19 DNA plasmid 	Inactivate the restriction enzyme. Incubate for 20 min at 65°C
3	<ul style="list-style-type: none"> • Promega Wizard SV and PCR kit 	Clean the sample
4	<ul style="list-style-type: none"> • BseYI-digested pUC19 DNA plasmid • Digoxigenin-ddUTP (1 mM) • dCTP (1 mM) • Klenow Fragment (5 U/μl) • Klenow buffer (10X) • MQ 	Sample labelling. Incubate at 37° C for 2 hours
5	<ul style="list-style-type: none"> • Promega Wizard SV and PCR kit 	Clean the sample
6	<ul style="list-style-type: none"> • Single-labelled pUC19 DNA plasmid • Bsal enzyme (10 U/μl) • 3.1 NEB buffer • MQ 	Single-labelled pUC19 DNA plasmid digestion. Incubate at 37°C overnight
7	<ul style="list-style-type: none"> • BSal-digested pUC19 DNA plasmid 	Inactivate the restriction enzyme. Incubate for 20 min at 65°C
8	<ul style="list-style-type: none"> • Promega Wizard SV and PCR kit 	Clean the sample
9	<ul style="list-style-type: none"> • BSal-digested pUC19 DNA plasmid • Biotin – ddUTP (1 mM) • dCTP (1mM) • dGTP (1mM) • Klenow Fragment (2 U/μl) • Klenow buffer (10X) • MQ 	Sample labelling. Incubate at 37° C for 2 hours

Table I: Two phase Klenow procedure to build a DNA construct ready for reconstitution

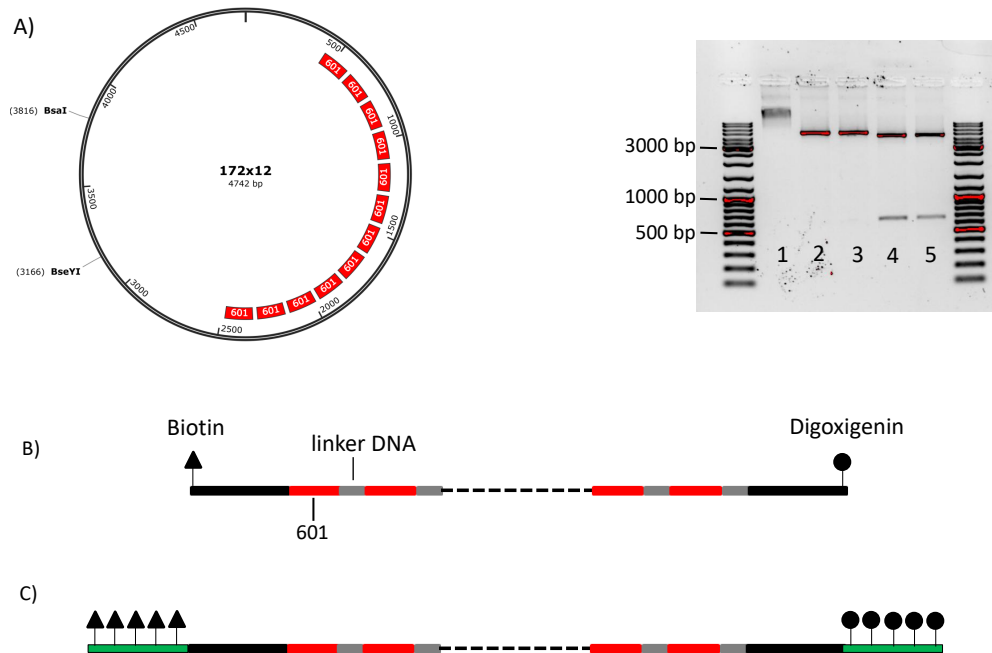


Figure 3.1: Procedure used in order to have a DNA construct ready for the re-constitution A) Example with 12 repeats of 601 Widow sequence for (pUC19) and gel for the plasmid digestion phase. We used a two phase Klenow procedure. Lane 1: Plasmid DNA (pUC19). Lane 2: 1st digestion by BseYI enzyme. Lane 3: 1st labelling with digoxigenin. Lane 4: 2nd digestion by BsaI enzyme. Lane 5: 2nd labelling with biotin. B) Product after the Klenow procedure. The red segments represent the repeated 601 Widow sequences and the grey ones the linker DNA. C) The torsionally constrained construct is made by ligating the construct with handles containing many biochemical linkers. The difference between the two constructs is that the one in B) is torsionally not constrained and the one in C) because of the long handles is torsionally constrained.

tubes floating in a beaker containing high salt buffer. A pump will slowly mix the high salt buffer with low salt buffer (1 x TE) effectively bringing down the salt concentration.

Figure 3.2 A depicts the lowering of the concentration of high salt buffer in the beaker. Two dimers of H3-H4 form a tetramer which wraps DNA. At lower salt the last two dimers H2A and H2B will bind to the construct, forming a nucleosome.

Figure 3.2 B shows a gel with the reconstituted chromatin. The first lane shows the plasmid DNA (pUC19) while the second lane shows the digested and labelled plasmid. Lanes 2 to 8 show the six reconstitutions made with different octamers-DNA ratios. The different band-shift between the six reconstitutions represents a titration, going from unsaturated to fully saturated fibers.

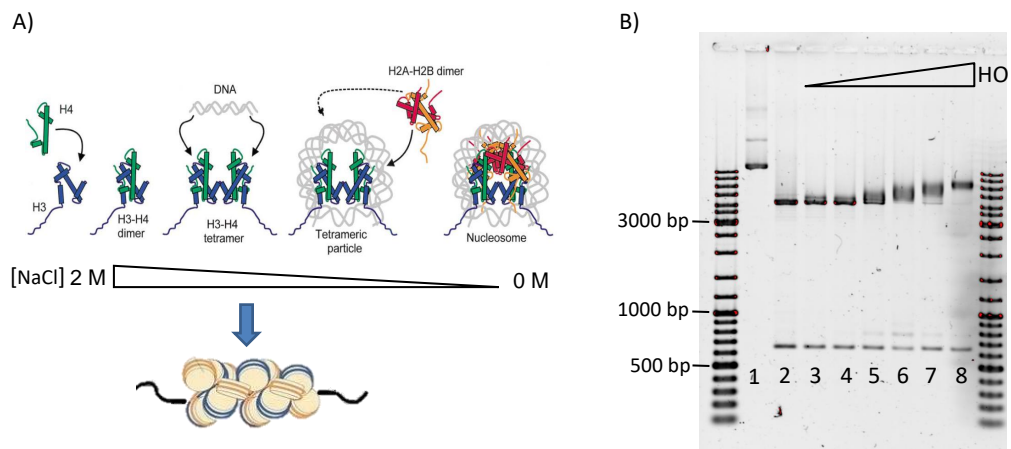


Figure 3.2: Reconstitution process. A) By decreasing the amount of high salt buffer in which the samples are, we induce a compaction of the various components present in the sample into the formation of a nucleosome B) Gel for the final reconstituted products. Lane 1: Plasmid DNA (pUC19). Lane 2: DNA digested with BseYI and BsaI enzymes and labelled with digoxigenin and biotine. Lane 3-8: titrations with six different octamers-DNA ratios 0:9, 1:1, 1:4, 1:6, 1:8 and 2:0.

3.2 Magnetic Tweezers

In figure 3.3 A we see that the set-up is composed by two magnets, an objective, a tube lens, a mirror and a CMOS camera.

The magnets induce a force on the magnetic bead that is attached to the chromatin fiber. In this way we will be able to manipulate the force exerted on the bead, and thus the stress applied on the chromatin fiber. The force on the beads is calibrated from magnet height with the following double exponential equation:

$$F = F_{MAX} \left(0.7 \exp \frac{-h}{L_1} + 0.3 \exp \frac{-h}{L_2} \right) + F_0 \quad (3.1)$$

Where $F_0=0.01$ pN, $L_1=1.4$ mm is the first decay length, $L_2=0.8$ mm the second decay length, $F_{MAX}=85$ pN and h represents the height of the magnet.

The bead is illuminated from the top with a collimated LED of wavelength $\lambda=595$ nm. Interference between incident and scattered light off the bead produces diffraction rings in the image plane of a CMOS camera. This effect is known as Lorenz-Mie scattering. At the bottom right of figure 3.3 A we see the resulting diffraction pattern, that changes with the height of the bead.

To extract the z-high of the bead we perform a cross correlation of the acquired image with computer-generated reference image which resembles the bead, yet contains only a single spatial frequency. The maximum of the cross correlation provides us with the XY position of the bead. The phase of the cross correlation at this position can be calibrated with z-position of the bead. Ultimately, the extension of the molecule is calculated from the phase shift of the 2D cross correlation at bead center. In figure 3.3 B we can see a force-extension curve for a DNA molecule. The curve is fitted with the WLC model.

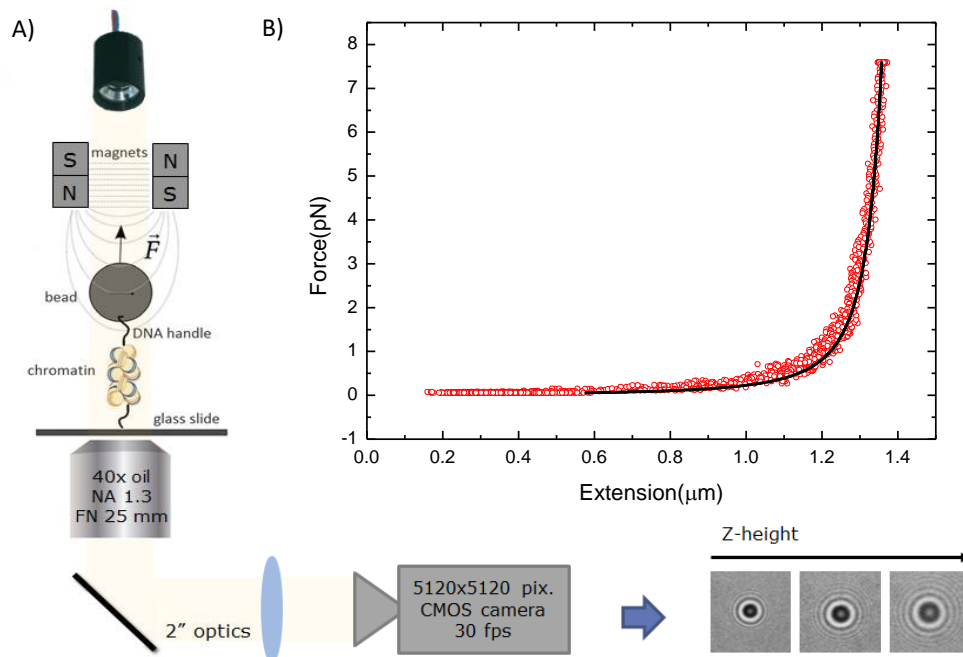


Figure 3.3: A) Scheme of the apparatus for the magnetic tweezers. A superparamagnetic bead with a diameter of $2.8 \mu\text{m}$ is attached to one of the ends of the chromatin fiber while the other one is attached to a glass surface. The magnetic field, created by the two magnets at the top of the apparatus, pulls the chromatin fiber in a controlled way. The objective under the glass surface tracks the changes in the interference pattern of each bead. A CMOS camera records the signal that will then be converted into variations in the z-height of the bead B) Example of typical bare DNA curve acquired with the apparatus (red circles) and the fit to a worm-like chain model (black line).

Results

In order to test how the variation of the linker length changes the fiber structure, we compared the 172 nucleosome repeat length (NRL) reconstituted chromatin with other NRL's three chromatin (see figure 4.1).

As an example we will evaluate the typical unfolding behaviour of a 167x15 NRL fiber in figure 4.1 A. Around 4 pN there is a transition where the extension increases while the force stays constant. Here the nucleosome-nucleosome interactions break and one turn of DNA around the nucleosomes is unwrapped. This transition is defined by the energy barrier ΔG_1 . Right after the first transition we can see another small extension. Then, as the force increases, we can see a zone containing steps. That is the force regime in which nucleosomes start to fully unwrap, leading to a behaviour of the construct that is very similar to that of bare DNA.

4.0.1 Comparison between chromatin fibers

The force-extension curves in figure 4.1 were fitted with a statistical mechanics model [5] that takes into account the contour length L , the number of nucleosomes n , the stiffness k , ΔG_1 and ΔG_2 . The last part of the graph represents double stranded DNA. We fitted a worm-like chain to the last part of the curve (solid black line), which overlaps perfectly. The black dotted lines represent worm-like chain fits of DNA with a contour length $L_0 - (n * 25 \text{ nm})$, where L_0 is the contour length of the DNA and 25 nm is the length gained when 86 base pairs unwrap from a nucleosome [5, 10].

While comparing the four graphs of figure 4.1 A-D we notice that the plateau at low force has a different shape for each of the graphs. This feature is more evident in figure 4.1 E-H, where zooms of figure 4.1 A-D at low forces are shown. For the 167 NRL fiber the plateau is very flat and

sharp, showing a cooperative unfolding of the fiber, in which all the nucleosomes of the fiber unstack simultaneously. For the 172 and 197 NRL fibers the plateau is less sharply defined, showing a continuous and gradual unwrapping of the nucleosomes forming the fiber. For the 202 NRL fiber the plateau is almost non-existent.

The force needed to fully unwrap the nucleosomes appears different for the four curves. This could be an indication of a different fiber structure. Moreover, we notice that the release curves (gray curves in figure 4.1) behave differently. For the 197 and 202 NRL fibers the release curves have a similar behaviour, returning at zero extension with a trajectory that never overlaps with the pulling one. In contrast, for the 172 NRL fiber we notice that the release curve overlaps with the pulling curve around the plateau area of the force-extension graph. This behaviour is clearer in figure 4.1 F. We can see a complete refolding of the fiber when released, and it is probably a sign that even if completely stretched, the 172 fiber does not lose its histones. Because each of those datasets were acquired with different pulling rates, it is difficult to compare the folding rates directly. Unfortunately we did not succeed in recording the release curve for the 167x15 NRL fiber.

Since the low force area of the graph contains the relevant information on the fiber structure we decided to further investigate the behaviour at low forces of the 172 NRL fiber up to a maximum force of 5.2 pN (figure 4.2 B and C). We especially wanted to examine if the first transition, the one characterized by ΔG_1 , is in equilibrium. Therefore we tested the reproducibility of our results at different pulling rates.

The two curves in figure 4.2 B and C are measured on the same molecule. However, they were acquired with a different pulling rate, i.e. the derivative of the force with respect of time, plotted in the inset of figure 4.2 D.

An important feature of those curves is that the pull and release curve of each graph have been acquired at the same pulling rate. figures B and C show that the pull and release curves perfectly overlap, showing that structural transitions in 172 fibers are in equilibrium below 6 pN. Figure 4.2 D shows the overlap of the curves in B and C. The fact that they overlap despite the different pulling rates demonstrates that in the low-force regime, we can compare measurements acquired with different pulling rates.

Table I shows the parameters ΔG_1 , ΔG_2 and k fitted for figure 4.2 B and C with their respective standard deviations. The fitted parameters confirm that the two curves in B and C have an almost identical behaviour.

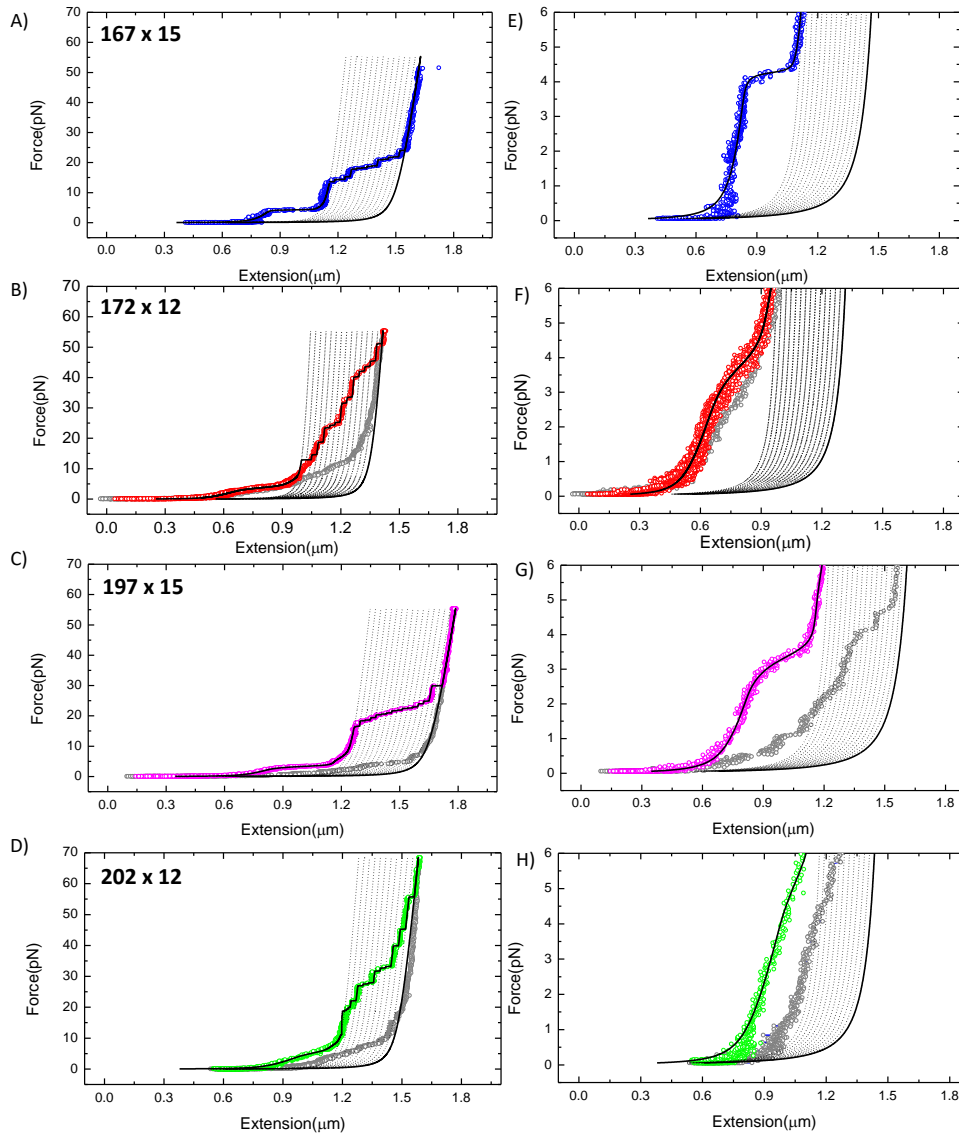


Figure 4.1: Folding fiber depends on variations of the linker length. In each graph we can distinguish three transitions. The first is where about one turn of DNA around the histones core is lost, at 4-5 pN. The second is the small extension after the first transition and the third, starting around 10-20 pN, in which steps are distinguishable, representing the total unwrapping of the DNA from the histones core. Notice the differences in the shape of the first transition, being sharper for the 167 then for the others. Also the force needed to unwrap the fiber is different between the graphs. Figures E-H show the difference with the refolding curve (in grey). Overlap with the pulling curve is only observed for the 172 fiber.

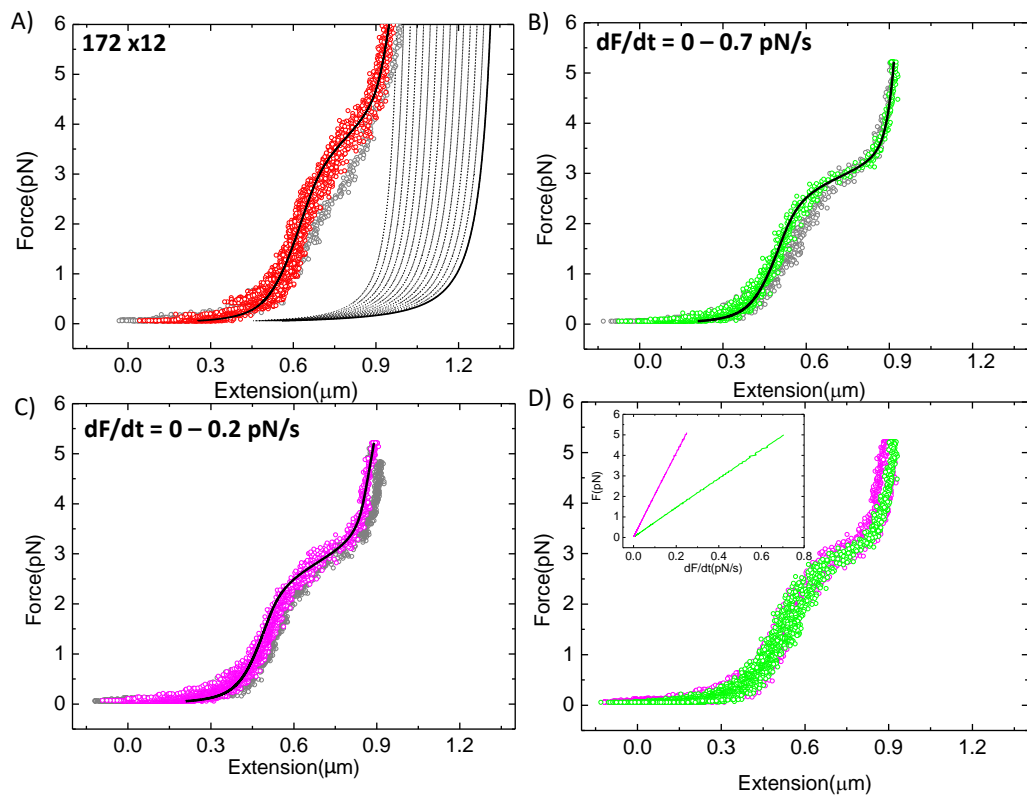


Figure 4.2: Low forces measurements are not affected by the pulling rate implying transitions in 172 NRL fibers are in equilibrium below 6 pN. A) Zoom at low forces from Figure 4.1 B B) Measurement taken with a pulling rate of 0 - 0.7 pN/s. C) Measurement of the same bead taken with a pulling rate of 0 - 0.2 pN/s. D) Overlap of the two different measurements B and C. They almost fully overlap, proving the fact that the pulling rate does not influence the behaviour of the fiber.

Table I: Fitted parameters

	Figure B	Figure C
ΔG_1	11.8 ± 0.06	11.6 ± 0.09
ΔG_2	4.1 ± 0.1	6.0 ± 0.2
K	0.3 ± 0.01	0.4 ± 0.01

4.1 Analysis

At forces > 6 pN, when the fiber has a beads-on-a-string conformation, the behaviour of each nucleosome is uncoupled. At lower forces however the rupturing of the fiber should depend on its folded structure. Figure 4.3 shows the three fitting parameters that describe this regime for chromatin fibers with four different NRL: 167x15, 172x12, 197x15, 202x12.

The number of measurements for each configuration (N) is much smaller for the 172 fiber compared to the others.

The stiffness characterizes the slope of the low force part of the force-extension graphs [5, 6]. At these forces the fiber is deformed by the pulling force exerted by the magnet, without breaking the interactions between the nucleosomes.

Figure 4.3 shows that the stiffness of the 167 NRL fiber has the highest value. This can also be seen in figure 4.1 E, in which the 167 fiber has the sharpest transition, resulting into a higher slope value. The 202 fiber has the lowest stiffness. Fitting this transition for the 202 construct was sometimes problematic because of the low slope values. Modelling the fiber as a stack of interacting nucleosomes, may not be valid in the case of the 202 NRL fiber. The 172 fiber has a stiffness similar to the 197 fiber, suggesting similar structures.

The fitted ΔG_1 parameter reveals two different values for the four fiber types. The 167 and 197 fibers have a high and similar ΔG_1 , indicating a solid and stable structure. In contrast, the 172 and 202 fibers have a low ΔG_1 , showing a less stable configuration.

ΔG_2 has a similar value for the 167, 197 and 202 fiber, while it seems to be slightly higher for the 172 construct.

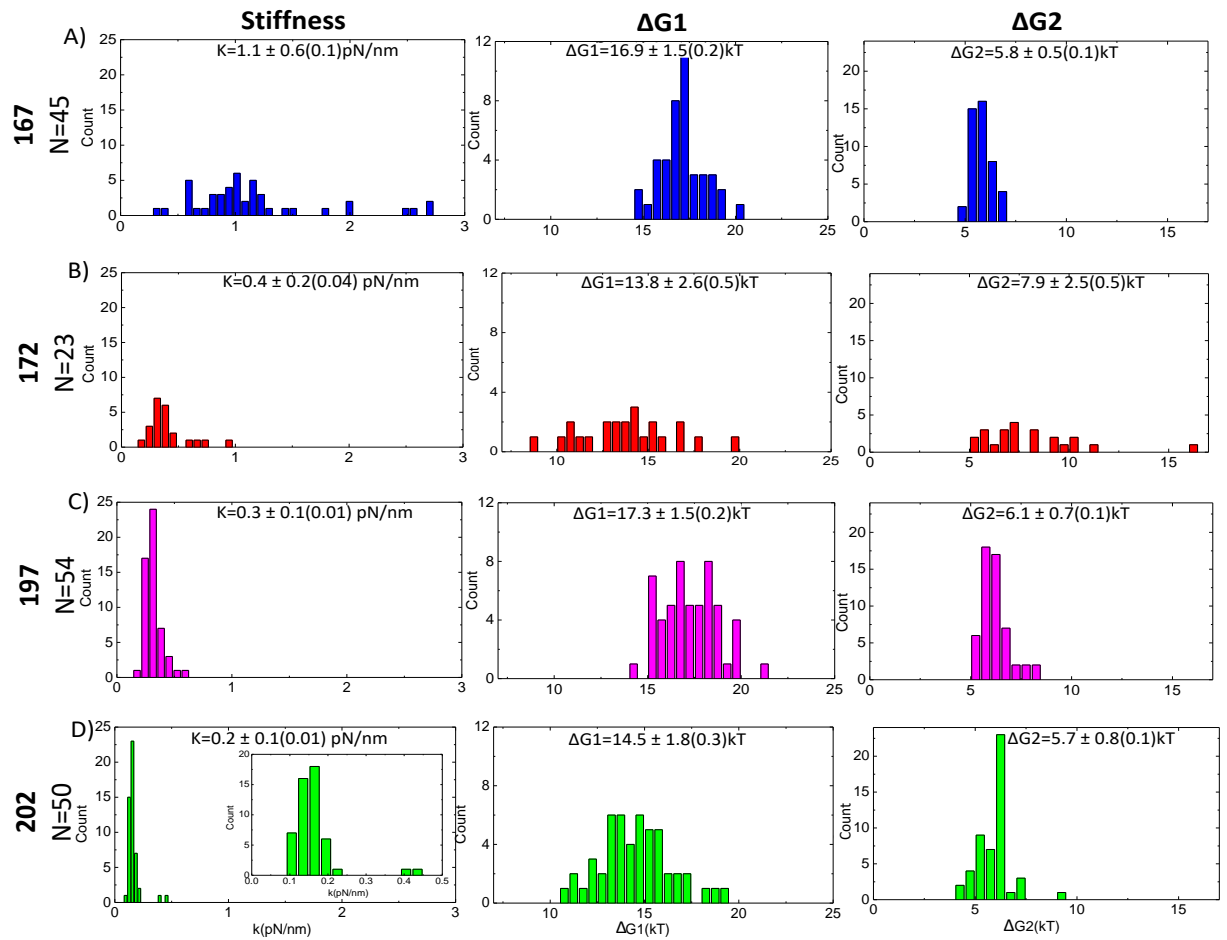


Figure 4.3: The stiffness for the 172 NRL fiber suggests a structure more similar to 197 NRL fibers than 167 NRL fibers. It has a lower ΔG_1 but a larger ΔG_2 compared to the others.

4.1.1 Torsionally free and torsionally constrained 172 NRL fibers

Since chromatin fibers are made by stacking nucleosomes wrapped by DNA, we anticipate that the addition of a torque and thus a torsional stress to the fiber affects the unfolding behaviour. To gain further knowledge into how the chromatin fibers are folded, we compared torsionally free and constrained fibers.

The torsionally constrained fiber has the same composition as the fiber shown in figure 3.1 B. However, this construct has long handles with multiple biotin and digoxigenin labels on each of them, impeding rotation of the DNA at the attachment points on the bead and the surface. This implies that it is not possible to release the torque builds up when pulling the fiber and unwrapping the nucleosomes. Figure 4.4 A and D show example of measurements taken with each 172 NRL fiber. Both can be fitted with the same statistical mechanics model.

Figure 4.4 C and F show the histograms for the stepsizes for each construct. In both case we obtained a stepsize of ± 25 nm for each unwrapped nucleosome, similar to previous studies[5, 10].

We quantified the stepsizes using a Student-t stepfinder algorithm and built the histograms at the stepsize. We fitted them calculating the cumulative distribution function (CDF).

$$F(s) = a_1 \left[1 + \operatorname{erf} \left(\frac{s - \mu}{\sigma \sqrt{2}} \right) \right] + a_2 \left[1 + \operatorname{erf} \left(\frac{s - 2\mu}{\sigma \sqrt{2}} \right) \right] \quad (4.1)$$

where s represents the stepsize, μ is the average value of the distribution and σ is its standard deviation. From the CDF we take the fitted μ and σ that we use to plot a double Gaussian (equation 4.2) on the histograms.

$$f(s) = A_1 \exp \frac{-(s - \mu)^2}{\sigma^2} + A_2 \exp \frac{-(s - 2\mu)^2}{\sigma^2} \quad (4.2)$$

The resulting double Gaussian distribution has two populations, one around 25 nm and another one around 50 nm. We attribute the large 50 nm stepsize to two simultaneous unwrapping events of 25 nm.

The two measurements in figure 4.4 A and D shows a similar behaviour. Both graphs show a smooth plateau around 4 pN and both have a release curve that overlaps with the plateau. Curiously the measurements for the 172 NRL torsionally constrained show a release curve immediately shifted to the left, indicating the fiber tends to refold faster than the not constrained fiber. Figures B and E show the behaviour of the fibers at low

forces. The shape of the first transition is the same for both the curves, but the force needed for the first transition to happen is higher for the torsionally free than for the torsionally constrained fiber. A relevant detail shown in figure 4.4 B and E is the difference in the release curve. Also at low forces the torsionally constrained fiber tends to refold faster than the torsionally free. The difference in the thickness of the curves is due to the different pulling rate used for the two measurements.

We further quantified the fraction of fully unfolded nucleosomes as a function of the applied force. Figure 4.4 G reveals the force needed to unwrap all the nucleosomes of the fiber for a large number of fibers. If the torsionally constrained fiber would indeed build up a higher torque when the nucleosomes unwrap we would expect a shift in the unwrapping force. However, for both types of fibers the force needed to unwrap 50% of the nucleosomes of the fibers is 25 pN. The torsionally free fiber appear to resist further unwrapping more than the torsionally constrained fibers, but taking into account that the dataset used for the torsionally free fibers was smaller than the one used for the torsionally constrained fibers, this effect may not be significant. It seems that the built-up torque does not have any effect on the last turn unwrapping of the nucleosomes.

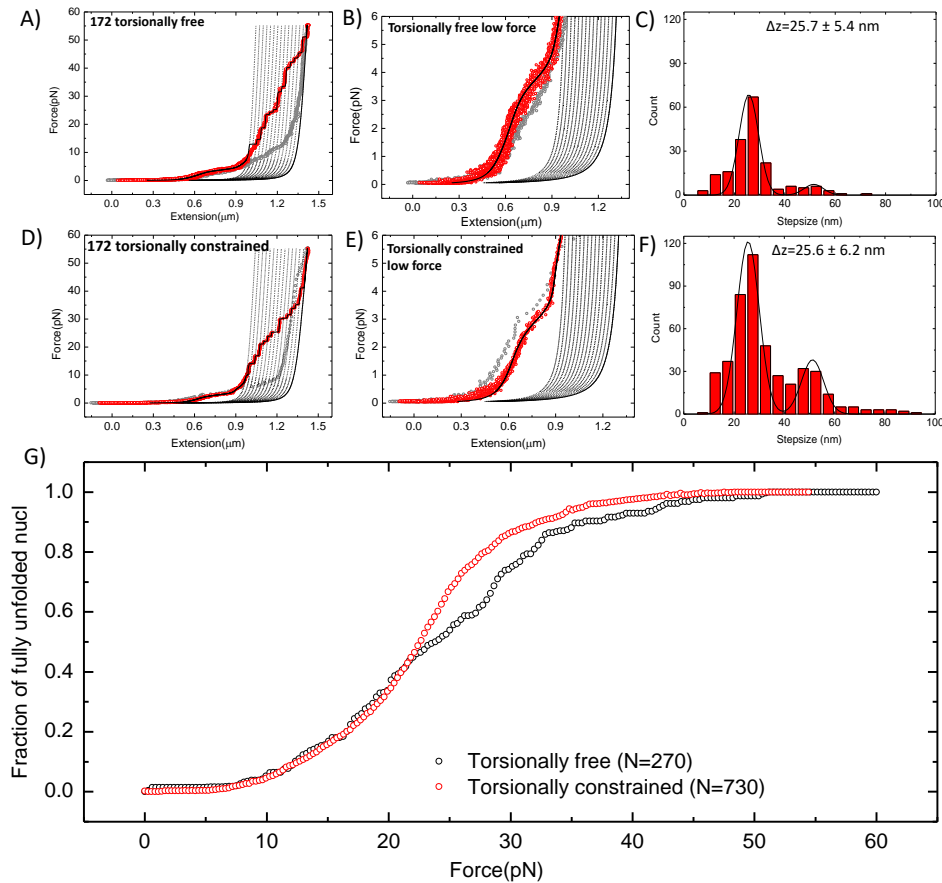


Figure 4.4: The second turn of unwrap is not affected by torsional stress. Curves for torsionally free (A) and torsionally constrained (D) fibers. In A) around 10 pN it is shown a Labview artifact in the fit of the curve. This is because most of the measurements for the 172 fiber have a slope after the plateau area that is very low compared to the range of expectation of the program. Zooms at low forces in B) and E) show that the shape of the plateau representing the first transition is very similar C) and F) stepsizes histograms fitted with a double Gaussian. G) Plot that compares how the two constructs unwrap when pulled by the magnetic tweezers.

4.2 192 NRL fiber

In addition to the experiments on the 172 NRL fiber, we have performed preliminary experiments on the 192 NRL construct, which might result in similar effects. The 192 NRL fibers have been reconstituted from pUC57 plasmid cut with *TatI* and *HgaI* enzymes using a two-phase Klenow procedure. Unfortunately, we do not have enough data to build a statistics for this fiber. In figure 5.2 we see an example of curve describing the behaviour of the 192 NRL reconstituted chromatin.

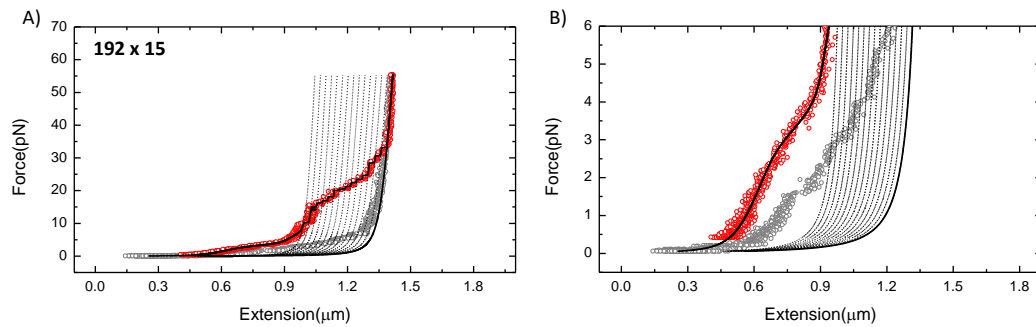


Figure 4.5: The 192 NRL fiber seems to show in the plateau a non cooperative transition at low forces (B). The release curve (in grey) shows hysteresis. Thus the first transition seems to be not in equilibrium.

We fitted the curve with the same statistical mechanics model used for the other fibers. From this fit we acquired those parameters:

$$\Delta G_1 = 12.6 \pm 1.4 \quad (0.6) \quad (4.3)$$

$$\Delta G_2 = 6.9 \pm 0.8 \quad (0.3) \quad (4.4)$$

$$k = 0.3 \pm 0.07 \quad (0.03) \quad (4.5)$$

where the errors are the standard deviation and numbers in parenthesis represents the SEM (standard error of the mean).

The stiffness is the same value as found for the 197 fiber. ΔG_1 is lower than the one for the other constructs (167, 172, 197 and 202 NRL), suggesting a much less stable fiber. When we compare it to the theoretical model in figure 2.5, we notice that the two do not match. In figure 2.5, the 45

bp linker construct does not have the lowest value. The reason could be that the 192 NRL fiber is just an array of non interacting nucleosomes, but this seems inconsistent with the obtained stiffness. Alternatively, it seems likely that the folded 192 NRL fiber stores an intermediate amount of free energy in twist of the linker DNA, which would destabilize the fiber, but not enough to impede nucleosome stacking in absence of force.

Hence, the theoretical results for long linkers would not have any physical meaning.

Chapter 5

Discussion

In previous studies [5–8] mechanical parameters and unfolding patterns have been linked to different higher-order structures. Specifically, the pattern of low-force transition reveal information on the structure: if the fiber dissociates cooperatively, or if it happens non-cooperatively. In chapter four we evaluated the force-extension graphs of four different chromatin fibers.

Previous studies [5, 6] have revealed a zig-zag structure for cooperative transitions, expressed by the sharp plateau at low forces by 167 NRL fibers, and a solenoid structure for not-cooperative transitions, shown for 197 NRL fibers. In contrast the plateau for the 202 NRL fiber in figure 4.1 is almost non-existent, suggesting that the 202 NRL fibers do not form a well-organized fiber structures, but rather an array of nucleosomes clustered together.

5.1 172 NRL fiber

The structure of the fiber with NRL 172 is still unknown. A hypothesis has been put forward by Nikitina et. al. In [14] they suggested 172 NRL fiber to have an anti-parallel zig-zag structure, but it has not been experimentally proven. Here, we performed force-spectroscopy to understand which type of structure the 172 NRL could form. Looking at figure 4.1 F we notice that the shape of the first transition for the 172 NRL fiber is not cooperative. The first transition of the 172 NRL fiber is very similar to the one shown by the 197 NRL fiber. Furthermore, from figure 4.3 we notice that the stiffness of the 172 NRL fiber is very similar to the one for the 197 NRL fiber, suggesting a solenoid structure for the two fibers.

Another interesting feature shown in figure 4.1 B and F is the shape of the release curve after stepsize unwrapping for the 172 NRL fiber. It overlaps with the plateau in the low-force regime. We see little hysteresis, conversely to what we see for the 197 fiber (compare figure 4.1 F and G). The presence of hysteresis in a transition reveals that refolding is slower than unfolding. This means that for the 172 NRL fiber the unfolding mechanism is reversible and that it is in equilibrium during the first transition, not experiencing any loss of energy.

When we compared data acquired with different pulling rates (figure 4.2), we notice that they overlap perfectly, leading to the conclusion that the pulling rate does not affect the behaviour of the fiber. Both the overlap of the two distinct curves and the overlap between the pull and release curves, confirm that the first transition in 172 NRL fibers is in equilibrium.

5.1.1 Torque effects on 172 NRL fibers

When a chromatin fiber is pulled, twist arises because of its intrinsically twisted conformation and because DNA unwraps from nucleosomes. When this twist cannot be dissipated, torque will build up.

After the first structural transition, the fibers is transformed in a chain of non-interacting single-wrapped nucleosomes. To understand this transformation we study the behaviour of the linker DNA. In the fiber configuration it is highly bent and twisted. Then, it is stretched into the beads-on-a-string configuration. At the same time that the linker DNA loses bending energy, it gains twist. To estimate the amount of twist added in the structure we evaluated the behaviour of a model that resembles a single nucleosome wrapped by DNA, shown in figure 5.1. It depicts the starting configuration: a single nucleosome wrapped with a single turn of DNA. Figure 5.1 A shows the position of the nucleosome in the solenoid fiber, horizontal compared to the fiber axis while figure 5.1 B shows a picture of the same configuration as in A but after having turned the wire for 180° counterclockwise. The image in B represents the position of the nucleosome in the bead-on-a-string configuration, vertical compared to the fiber axis. We have shown that pulling the fiber from a solenoid to a beads-on-a-string configuration adds 180° of twist in the linker DNA.

The 172 NRL fibers were composed of 12 nucleosomes. Thus, each nucleosome adds a twist of 180° to the total structure when stretched. A torsionally free DNA construct such as the one with single biotin and digoxigenin labels at the edges can freely rotate at the biotin-end. The torsionally constrained DNA construct cannot do the same, and therefore we

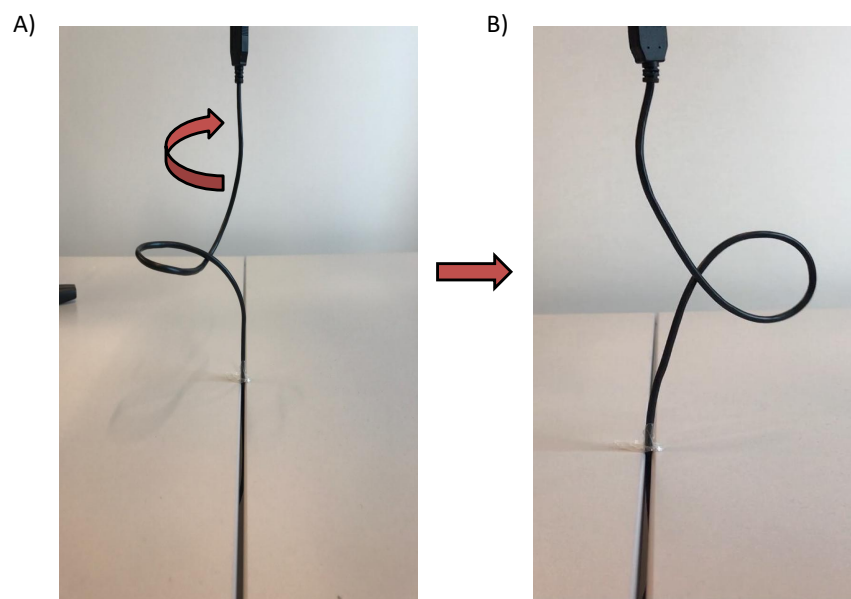


Figure 5.1: When the transition takes place a twist of π is added to the structure through the linker DNA. A) Simplification of a nucleosome in the solenoid structure B) Result after turning the wire 180° . The nucleosome changed orientation from horizontal to vertical. This implies the addition of a 180° twist during the first fiber transition in the linker DNA.

expected a difference between the fibers response. In figure 4.4 we compared the behaviours of the torsionally free and constrained fibers. From both the force-extension curves and the histograms in figure 4.4 we notice that the two fibers express a similar behaviour. The force-extension curves show the first transition happening at a similar force and for both fibers the refolding curve overlaps with the pulling curve at the same high. Moreover, the histograms show an almost identical value for the stepsizes. Figure 4.4 G shows the force needed to unwrap all the nucleosomes present in the fiber for both constructs. Also there, the response of the two constructs is similar. Therefore, we can conclude that the induced torque has negligible effect on the fiber behaviour. This could happen if the linker DNA in the stacked fiber is somewhat pre-twisted. So it compensates for the twist that is released when unstacking.

5.2 Does the experimental ΔG_1 agree with theory?

ΔG_1 represents the sum of nucleosome-nucleosome interaction (positive), twist stress (negative), bending stress (negative) introduced in the DNA linker and unwrapping energy (negative) necessary to release part of the bending and twist stress stored. We have calculated a simplified theoretical ΔG_1 (see figure 2.5) for solenoid structures with different linker lengths for the two extreme limits 0° and 180° twist. Here, we will focus on the 197 NRL fiber, hypotized in [5] to have a solenoid structure, and on the 172 NRL fiber. These fibers seem to have a similar structure as the stiffness has the same magnitude.

Comparing the theoretical results with the experiments (figure 4.3) for the 172 and 197 NRL fibers, we notice that the experimental results qualitatively agree with the theoretical ΔG_1 calculated for 0° twist. An important aspect of the model is that nucleosomes in 197 NRL fiber are partially unwrapped. The analysis in figure 4.3 shows for the 172 NRL fiber the lowest ΔG_1 . The curves describing a ΔG_1 of the 172 NRL fiber are lower than the one for the 197 NRL fiber because the 172 NRL only needs limited bending of the linker DNA and does not require unwrapping. This is a new hypothesis that could be tested by FRET experiments. This partially matches with the experiments. The values of ΔG_1 for 172 and 197 NRL fibers lay around 10 and 20 $k_B T$, while in figure 2.5 for 0° twist the curves in the area of interest lay between ± 12 and $\pm 25 k_B T$, a much broader range. The not perfect correspondence between theory and experiments could be because

we only analysed two extremes of linker twists.

Of course our model is so simplified that more subtle effects cannot be described, and a better analysis would require more refined structural modelling. Our analysis suggests however that the 197 NRL solenoid fiber stores a little twist in its linker DNA before it undergoes the next transition, governed by ΔG_2 .

Conclusion

Chromatin is found in all eukaryotes and it consists in a complex of macromolecules such as DNA and proteins. This complex of macromolecules is fundamental for the packing of DNA inside cells, yet its structure remains poorly understood.

Here, we addressed if variations of linker DNA affect structural changes in chromatin fibers. The results have shown that fibers with different linker DNA length respond differently to force spectroscopy. Specifically we looked at their behaviour at low forces, where fibers experience the first structural transitions. We distinguish between different fibers according to the value of the stiffness fitted at low forces. Fibers with a low stiffness and a non-cooperative transition are attributed to solenoid structure. A high stiffness and a cooperative behaviour are attributed to zig-zag structure. The 172 NRL fiber has a behaviour similar to the 197 NRL fiber, indicating that the 172 NRL fiber could be a solenoid.

Furthermore, we investigated the difference in the behaviour of torsionally constrained fibers. We deduced that the induced torque at high forces is negligible.

A future improvement towards a full understanding of the low-force behaviour of the fibers could be the development of a mathematical model to describe the first transition of a zig-zag fiber. Having a theoretical model to describe the ΔG_1 energetic barrier will help to interpret our experimental data. This could lead to a more refined chromatin structural modelling, that will support the exploration of DNA unwrapping in fibers and the role of twist, torque and bending of linker DNA.

Evaluation of single bp steps in nucleosome arrays would be instrumental in understanding the higher order structure of chromatin fibers. Moving in that direction, continuing to study the 192 NRL fiber behaviour

will give a broader insight in the future studies on the subject.

Although vital, chromatin remains an elusive structure. Every step will bring us closer in understanding this building block of life.

Bibliography

- [1] Gary Felsenfeld, Mark Groudine. *Controlling the double helix*. Nature, 2003.
- [2] Ralf Blossey, Helmut Schiessel. *The dynamics of the nucleosomes: thermal effects, external forces and ATP*. FEBS Journal, 2011.
- [3] John F. Marko, Simona Cocco. *The micromechanics of DNA*. Physics World, 2003.
- [4] John F. Marko, Eric D. Siggia. *Stretching DNA*. Macromolecules, 1995.
- [5] He Meng, Kurt Andresen, John van Noort. *Quantitative analysis of single-molecule force spectroscopy on folded chromatin fibers*. Nucleic Acids Research, 2015 .
- [6] Maarten Kruithof, Fan-Tso Chien, Andrew Routh, Colin Logie, Daniela Rhodes, John van Noort. *Single-molecule force spectroscopy reveals a highly compliant helical folding for the 30-nm chromatin fiber*. Nature America, 2009.
- [7] Nick Kepper, Dietrich Foethke, Rene Stehr, Gero Wedemann, Karsten Rippe. *Nucleosome geometry and internucleosomal interactions control the chromatin fiber conformation*. Biophysical Journal, 2008.
- [8] Helmut Schiessel. *The physics of chromatin*. Journal of Physics : Condensed matter, 2003.
- [9] Philip J.J. Robinson, Louise Fairal, Van A.T. Huynh, Daniela Rhodes. *EM measurements define the dimensions of the "30-nm" chromatin fiber: Evidence for a compact, interdigitated structure*. PNAS, 2006.

- [10] Fan-Tso Chien, John van Noort. *10 Years of tension on chromatin: Results from single molecule force spectroscopy*. Current pharmaceutical biotechnology, 2009.
- [11] Van A.T. Huynh, Philip J.J. Robinson, Daniela Rhodes. *A method for the In Vitro reconstitution of a defined "30 nm" chromatin fibre containing stoichiometric amounts of the linker histone*. Journal of Molecular Biology, 2005
- [12] P.T. Lowary, J. Widom *New DNA sequence rules for high affinity binding to histone octamer and sequence-directed nucleosome positioning*. Journal of Molecular Biology, 1998
- [13] Andrew Routh, Daniela Rhodes. *n vitro reconstitution of nucleosome arrays with a stoichiometric content of histone octamer and linker histone (PROT42)*. 2009
- [14] Tatiana Nikitina, Davood Norouzi, Sergei A. Grigoryev, Victor B. Zhurkin. *DNA topology in chromatin is defined by nucleosome spacing*. bioRxiv, 2017
- [15] Harry R. Matthews. *DNA Structure Prerequisite Information*. Biology Concept and Connections, 1997
- [16] C.L. Huskins. *Mitosis and Meiosis*. Nature, 1933
- [17] H. Sellou, T. Lebeaupin, C. Chapuis, R. Smith, A. Hegele, H.R. Singh, M. Kozlowski, S. Bultmann, A.G. Ladurner, G. Timinszky, S. Huet. *The poly(ADP-ribose)-dependent chromatin remodeler Alc1 induces local chromatin relaxation upon DNA damage*. Molecular Biology of the Cell, 2016
- [18] M.C. Barton, A. J. Crowe. *Chromatin alteration, transcription and replication: What's the opening line to the story?*. Oncogene, 2011
- [19] K. Luger, M. L. Dechassa, D.J. Tremethick. *New insights into nucleosome and chromatin structure: an ordered state or a disordered affair?*. Nature reviews. Molecular cell biology, 2012
- [20] Jing Jin, Lu Bai, Daniel S Johnson, Robert M Fulbright, Maria L Kireeva, Mikhail Kashlev, Michelle D Wang. *Synergistic action of RNA polymerases in overcoming the nucleosomal barrier*. Nature structural and molecular biology, 2010
- [21] K. Luger, A.W. Ma, R.K. Richmond, D.F. Sargent, T.J. Richmond. *Crystal structure of the nucleosome core particle at 2.8 Å resolution*. Nature, 1997

-
- [22] S.J. Correl, M.H. Shubert, S.A. Grigoryev. *Short nucleosome repeats impose rotational modulations on chromatin fiber folding*. EMBO, 2012
- [23] Davood Norouzi, Ataur Katebi, Feng Cui, Victor B. Zhurkin. *Topological diversity of chromatin fibers: Interplay between nucleosome repeat length, DNA linking number and the level of transcription*. AIMS Biophysics, 2015